

## Silicon carbide reinforced vertically aligned carbon nanotube composite for harsh environment mems

Mo, Jiarui; Shankar, Shreyas; Zhang, Guoqi ; Vollebregt, Sten

**DOI**

[10.1109/MEMS49605.2023.10052162](https://doi.org/10.1109/MEMS49605.2023.10052162)

**Publication date**

2023

**Document Version**

Final published version

**Published in**

Proceedings of the 2023 IEEE 36th International Conference on Micro Electro Mechanical Systems (MEMS)

**Citation (APA)**

Mo, J., Shankar, S., Zhang, G., & Vollebregt, S. (2023). Silicon carbide reinforced vertically aligned carbon nanotube composite for harsh environment mems. In *Proceedings of the 2023 IEEE 36th International Conference on Micro Electro Mechanical Systems (MEMS)* (pp. 72-75). IEEE.  
<https://doi.org/10.1109/MEMS49605.2023.10052162>

**Important note**

To cite this publication, please use the final published version (if applicable).  
Please check the document version above.

**Copyright**

Other than for strictly personal use, it is not permitted to download, forward or distribute the text or part of it, without the consent of the author(s) and/or copyright holder(s), unless the work is under an open content license such as Creative Commons.

**Takedown policy**

Please contact us and provide details if you believe this document breaches copyrights.  
We will remove access to the work immediately and investigate your claim.

***Green Open Access added to TU Delft Institutional Repository***

***'You share, we take care!' - Taverne project***

**<https://www.openaccess.nl/en/you-share-we-take-care>**

Otherwise as indicated in the copyright section: the publisher is the copyright holder of this work and the author uses the Dutch legislation to make this work public.

# SILICON CARBIDE REINFORCED VERTICALLY ALIGNED CARBON NANOTUBE COMPOSITE FOR HARSH ENVIRONMENT MEMS

Jiarui Mo, Shreyas Shankar, Guoqi Zhang, and Sten Vollebregt

Laboratory of Electronic Components, Technology and Material (ECTM), Department of Microelectronics, Delft University of Technology, Delft, The Netherlands

## ABSTRACT

Fabricating high-aspect-ratio (HAR) structures with silicon carbide (SiC) is a challenging task. This paper presents a silicon carbide (SiC) reinforced vertically aligned carbon nanotubes (VACNT) composite as a promising candidate to fabricate HAR MEMS devices for harsh environment applications. The use of a VACNT array allows the fast realization of HAR structures as a template for MEMS fabrication. The template can later be easily filled by amorphous-SiC due to the porous nature of the VACNT forest. The SiC-CNT nanocomposite has electrical properties dominated by VACNT arrays and mechanical stability dominated by the a-SiC. Based on this concept, a thermal actuator is fabricated and proven to function up to 450°C for the first time.

## KEYWORDS

SiC-CNT composite, HAR structures, harsh environment, thermal actuator

## INTRODUCTION

With the advancement of the micro-/nano-fabrication technology, M-/NEMS devices play a significant role in various fields. For instance, many silicon (Si) MEMS devices have been applied to automotive products. In recent years, MEMS devices have been increasingly needed in high-temperature environments, for instance, oil drilling, combustion monitoring, and aerospace applications. However, Si-based MEMS can hardly meet the requirement as silicon's electrical and mechanical properties experience degradations at elevated temperatures.

SiC, a well-known wide bandgap semiconductor, has numerous advantages over Si. SiC has higher thermal conductivity, high critical E-field, high chemical inertness, and high Young's modulus. Thanks to the wide bandgap, SiC-based active devices maintain electrical behaviors above 300°C, which is the temperature limit of Si-based active devices. Most importantly, SiC is not plastically deformable even at elevated temperatures above 500°C. These properties are favourable for designing robust MEMS devices for harsh environments. Researchers have put much effort into SiC MEMS sensor development in recent years. These sensors include but are not limited to pressure sensors [1, 2, 3, 4], motion sensors [5, 6, 7], and resonators [8, 9, 10, 11, 12]. Currently, SiC MEMS development is limited by insufficient micro-machining techniques. Due to the mechanical and chemical stability of the SiC, traditional etching methods are not efficient. Typically, the SiC etching rate by dry etching is below 1  $\mu\text{m}/\text{min}$ . In 2021, Erbacher et al. reported the highest etching rate (4  $\mu\text{m}/\text{min}$ ) so far by reactive ion etching (RIE) with  $\text{SF}_6/\text{O}_2/\text{He}$  gas mixture [13]. However, this etching

rate is still relatively low compared to Si bulk etching method, and it requires a particular inductively coupled plasma (ICP) etcher with high power density. In addition to the slow etch rate, rough etching surface, non-vertical sidewalls, and micro-trenching effect are often observed in the literature [14, 15, 16].

The CNT forrest in combination with various filler materials is an attractive material for MEMS applications [17,18]. In this work, we propose using SiC-CNT composite as an alternative for the fast fabrication of HAR structure. VACNT arrays can be grown at a high growthrate (a few tens of micrometers per minute) while maintaining a vertical sidewall, and HAR structures can be obtained easily with the array. After the growth, the porous HAR template can be filled by LPCVD SiC; therefore, the mechanical property of the array is reinforced by SiC [19]. To demonstrate the potential of this composite thermal actuators were fabricated and tested up to 450°C.

## SIC-CNT COMPOSITE

### Fabrication of the composite

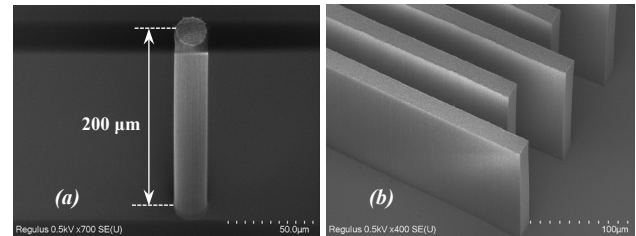


Figure 1: As-deposited HAR VACNT (a) pillars; (b) blocks from a 30° tilted view.

The fabrication of the composite consists of only a one-mask step, i.e. the patterning of the catalyst. First, an oxide layer is thermally grown, acting as a diffusion barrier from the metal catalyst to the Si substrate [17]. Then  $\text{Al}_2\text{O}_3$  (20 nm) and Fe (2 nm) layers are evaporated by a lift-off process. The CNT growth is performed with an Aixtron Blackmagic CVD system. The precursor gases are  $\text{C}_2\text{H}_2/\text{H}_2$  (50/700 sccm), reacting at 80 mbar and 600°C. After the CNT growth, the sample is loaded into an LPCVD furnace for SiC deposition. The SiC deposition is done with

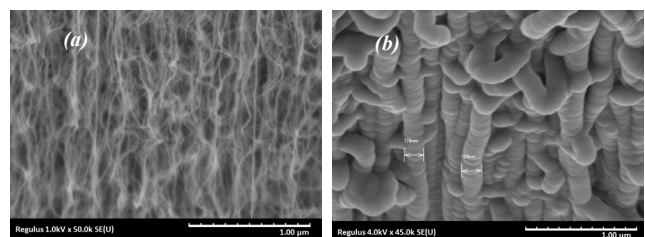


Figure 2: CNT array (a) before and (b) after being coated by a-SiC.

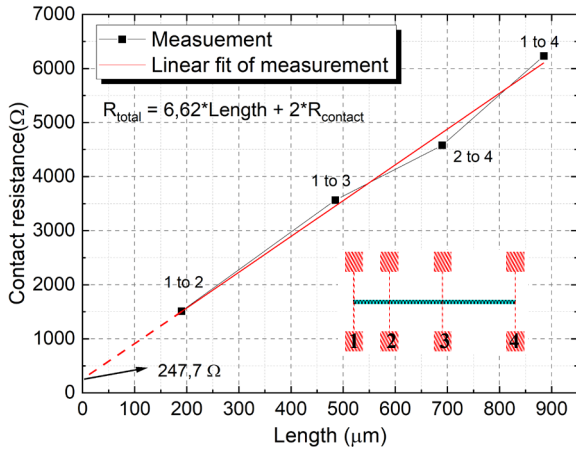


Figure 3: Measured resistances from different segments of the TLM structure. The intersection between the curve and y-axis is the value of the contact resistance.

$\text{SiH}_2\text{Cl}_2$  and  $\text{C}_2\text{H}_2$  diluted in  $\text{H}_2$  at  $760^\circ\text{C}$  at 1 mbar.

Figure 1 shows as-deposited CNT pillars and blocks with a maximum aspect ratio of 10. Figure 2a and Figure 2b provide close-up views of the CNT array surface before and after the SiC deposition. As can be observed, the CNTs are densified by the SiC and are not only weakly bonded by van der Waals force.

### Electrical properties of SiC-CNT composite

In many MEMS applications, the construction material is required to be conductive. Examples are capacitive accelerometers, thermal actuators, and resonators. However, the filler material, i.e. amorphous SiC, is non-conductive. Therefore, it is essential to investigate the bulk resistivity of the composite. In addition, as the device needs to interface with the instrument/readout, the contact resistance from composite to metal is also characterized. For this purpose, resistors with different dimensions and test structures for the transmission line method (TLM) were fabricated to evaluate the bulk resistivity of the SiC-CNT composite and the contact resistance. To measure the test structure, a metal layer was sputtered and patterned as electrodes before fabricating SiC-CNT. Titanium nitride (TiN) was used because it provides sufficient thermal budget for the subsequent process.

The resistivity of the composite is extracted and summarized in Table 1. The resistivity of the measured samples ranges from  $6.84 \times 10^{-3}$  to  $7.09 \times 10^{-3} \Omega \cdot \text{m}$ . The resistivity of the intrinsic VACNT is  $2.23 \times 10^{-3} \Omega \cdot \text{m}$ , which shows better conductivity than the SiC-CNT composite. Nevertheless, the conductivity of the composite still shows an improvement of a few orders of magnitude compared to a-SiC ( $\sim \text{M}\Omega \cdot \text{cm}$ ). Hence, it implies that the

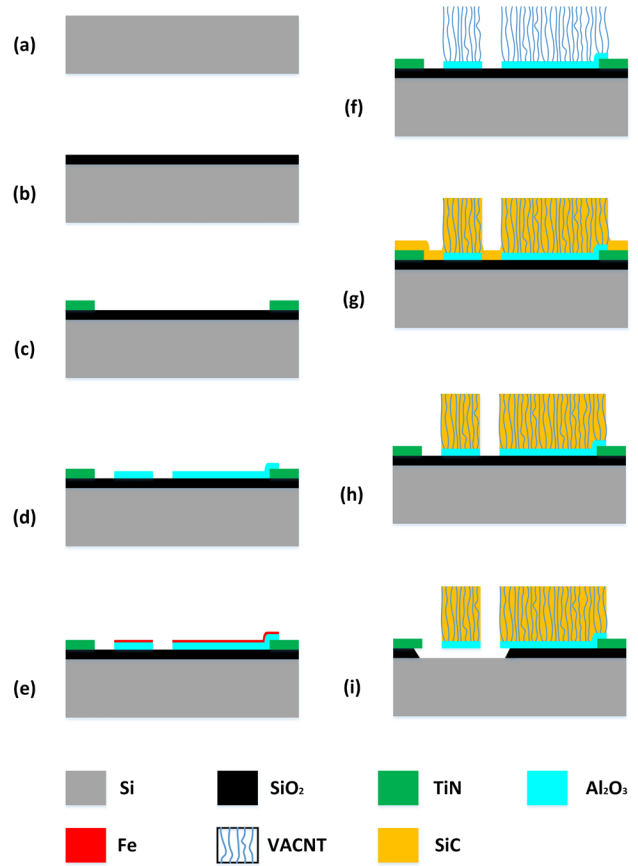


Fig. 4. Process overview of the SiC-CNT composite. (a) Si substrate is used as starting material; (b)  $\text{SiO}_2$  sacrificial layer is deposited; (c) TiN is sputtered as electrodes; (d)(e)  $\text{Al}_2\text{O}_3/\text{Fe}$  bilayer is evaporated, and the patterning of the bilayer is done by lift-off process; (f) CNT arrays are grown on the area defined by Fe; (g) The CNT array is infiltrated by a-SiC; (h) Floor layer removal by dry etching; (i) Vapor HF to release the structure.

conductive paths between individual CNTs remain and dominate the electrical behaviour of the composite.

The TLM measurement result is given in Figure 3. The intersection between the linear fit and y-axis is the resistance between a  $20 \times 10 \mu\text{m}^2$  TiN/SiC-CNT interface. The resulting specific contact resistivity is  $2.48 \times 10^{-4} \Omega \cdot \text{cm}^2$ .

### SIC-CNT THERMAL ACTUATOR

A thermal actuator is fabricated and characterized as a demonstrator of using the SiC-CNT composite as an emerging material for MEMS applications.

#### Fabrication of the thermal actuator

The process flow of the thermal actuator is illustrated in Figure 4. Since the thermal actuator requires a suspended

Table 1. Resistance measurement of SiC-coated CNTs resistors(\* This sample is not coated with a-SiC)

Sample (#)	CNT Height ( $\mu\text{m}$ )	Width ( $\mu\text{m}$ )	Resistance ( $\Omega$ )	Resistivity ( $\Omega \cdot \text{m}$ )
1	10	10	20540	0.00684
2	10	20	10580	0.00705
3	10	40	5321	0.00709
4	20	10	10610	0.00707
5*	33	10	2030	0.00223

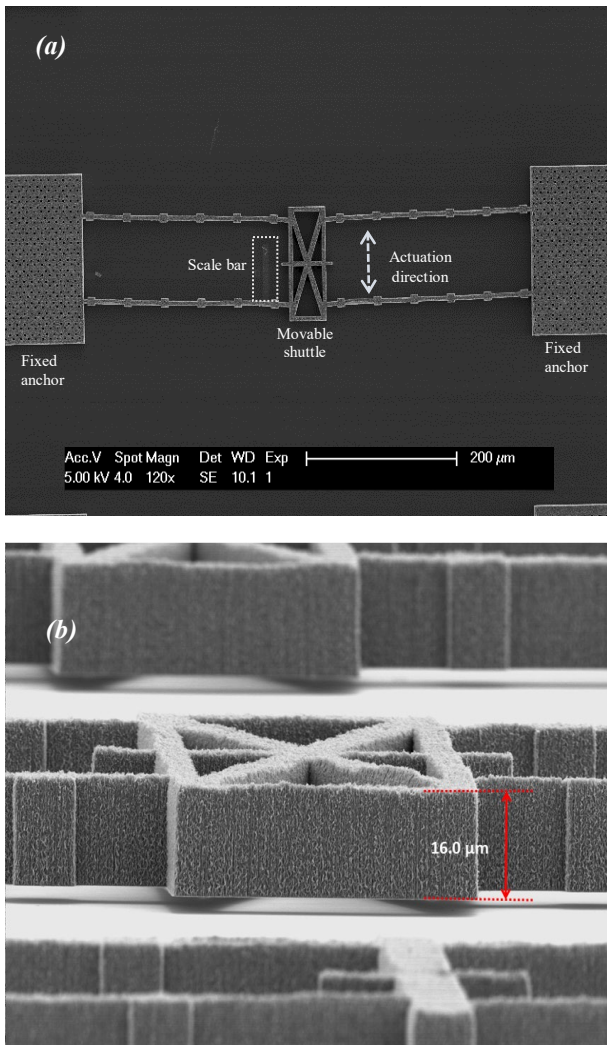


Figure 5: (a) A complete view of the thermal actuator based on SiC-CNT composite; (b) A zoom-in view of the suspended shuttle.

structure for actuation, SiC-CNT composite fabrication process is incorporated with a surface micro-machining process. The process starts with a 100 mm Si wafer (Figure 4a). First, a 3 μm thermal oxide is grown on the substrate as the sacrificial layer (Figure 4b). Then, Ti/TiN is sputtered and patterned, acting as electrodes for the device (Figure 4c). Figure 4d to 4g describe the fabrication of SiC-CNT composite, which is the same process as mentioned earlier. Before releasing the SiC-CNT structure, the SiC floor layer needs to be removed by dry etching. This is not only to make sure that the sacrificial layer can be exposed to the etchant, but also to ensure proper probing of the metal pad during measurement. The final release is done by vapour HF so that the risk of stiction can be eliminated.

The final device is demonstrated in Figure 5. The actuator consists of two fixed anchors, one movable shuttle, and suspended beams. The beams are designed to be pre-bended to a certain direction, which determines the actuation direction. From Figure 5b, it can be seen that the movable shuttle is suspended without sagging after being released.

### Device characterization

The actuator is first tested at room temperature. The

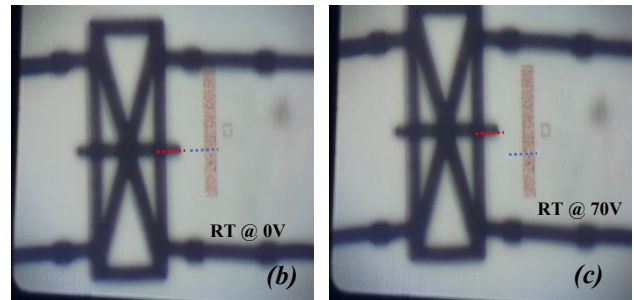
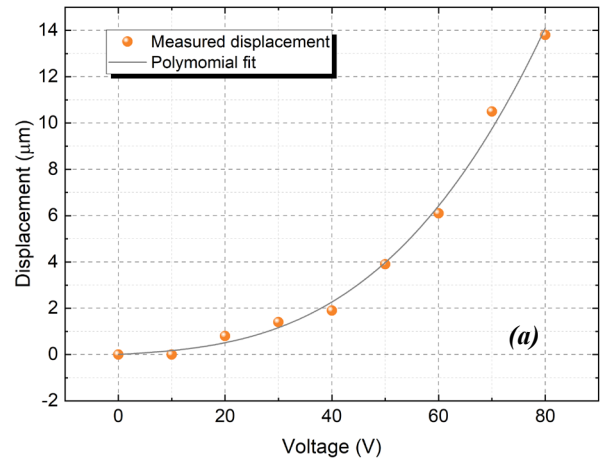


Figure 6: (a) The displacement of the movable shuttle vs.  $V_{bias}$ ; (b) The actuator at rest position at 25°C (0 V); (c) The device is actuated by 70 V bias at 25°C

device is biased at different voltages ( $V_{bias}$ ), from 0 to 80 V, with a step of 10 V. The Joule heat generated on the device will induce thermal expansion, resulting in a displacement towards the pre-bended direction. The movement of the movable shuttle is read by a scale bar fabricated alongside the shuttle. The displacement as a function of the bias voltage is plotted in Figure 6a. The  $V_{bias}$  and displacement relationship aligned well with a third-order polynomial fit. The movement can hardly be seen until  $V_{bias}$  reaches 20 V. The maximum displacement is around 13.8 μm, obtained at 80 V. It is worth mentioning that the device breaks down when  $V_{bias}$  is approximately 90 V due to the excessive Joule heating.

To verify the high-temperature stability of the composite and the thermal actuator, we measured the device at elevated temperatures, i.e. at 150°C, 300°C, and 450°C. The biasing voltage was set to 70 V to avoid the breakdown of the device due to the external heat source in combination with self-heating. In fact, the breakdown voltage decreases to around 80 V when the ambient temperature rises to 450°C. Figure 7a to 7c demonstrate the thermally-induced displacement, i.e. 9.4 μm (150°C), 11.0 μm (300°C), and 9.9 μm (450°C). The displacement did not show a significant change compared to actuation at room temperature (10.5 μm). Figure 7d shows that the rest position at 450°C is almost the same as that at room temperature; therefore, it can be concluded that the external heat source does not contribute much to the thermal actuation temperature. The reason could be that the SiC-CNT composite has a similar coefficient of thermal expansion (CTE) so that the device expand to a similar extent as the Si substrate.

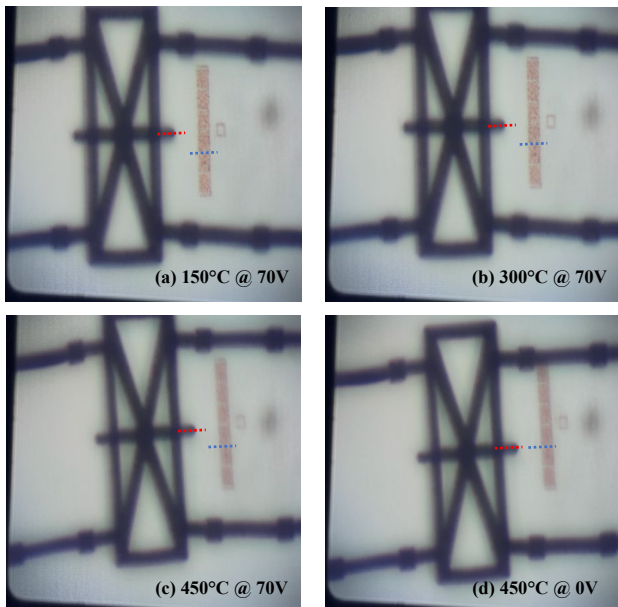


Figure 7: The thermal actuator biased at 70 V at (a) 150°C, (b) 300°C, and (c) 450°C; (d) The shuttle returned to rest position, showing no plastic deformation.

The high-temperature measurement result shows that the thermal actuator can work properly at 450°C, and the SiC-CNT composite showed stable mechanical properties at the same temperature. It needs to be mentioned that the device can possibly work at a higher temperature as the measurement setup was limited to 450°C.

## CONCLUSION

In this paper, we presented a generic fabrication technique for harsh-environment applications. The method uses the SiC reinforced VACNT array, enabling fast fabrication of SiC-based HAR structures. It is proven that the electrical behavior of the SiC-CNT composite is dominated by CNT.

The fabrication process of the composite can be incorporated into standard process techniques, such as the surface micromachining process. To illustrate this, a thermal actuator was fabricated and characterized. The device showed stable operation at 450°C successfully, and the composite can potentially withstand an even higher temperature without degradation. The result shows that the SiC-CNT composite can be used as an alternative for SiC for harsh environment MEMS design.

## REFERENCES

- [1] L. M. Middelburg et al., "Toward a Self-sensing Piezoresistive Pressure Sensor for All-SiC Monolithic Integration", *IEEE Sensors Journal*, vol. 20, pp. 11265-11274, 2020.
- [2] J. Mo et al., "Surface-micromachined Silicon Carbide Pirani Gauges for Harsh Environments", *IEEE Sensors Journal*, vol. 21, pp. 1350-1358, 2020.
- [3] H-P. Phan et al., "Highly sensitive pressure sensors employing 3C-SiC nanowires fabricated on a free standing structure", *Materials & Design*, vol. 156, pp. 16-21, 2018.
- [4] R. S. Okojie et al., "4H-SiC Piezoresistive Pressure Sensors at 800°C with Observed Sensitivity

- Recovery", *IEEE Electron Device Letters*, vol. 36, pp. 16-21, 2018.
- [5] S. Rajgopal et al., "A Silicon Carbide Accelerometer for Extreme Environment Applications", *Materials Science Forum*, vol. 600, pp. 859-862, 2009.
- [6] A. Alfaifi et al., "Optimization of In-plane SiC Capacitive Accelerometer Design Parameters", in *2016 14th IEEE International New Circuits and Systems Conference (NEWCAS)*, Vancouver, June 26-29, 2016, pp. 1-4.
- [7] A. R. Atwell et al., "Simulation, Fabrication, and Testing of Bulk Micromachined 6H-SiC High-g Piezoresistive Accelerometer", *Sensors and Actuators A: Physical*, vol. 104, pp. 11-18, 2003.
- [8] K. Adachi et al., "Single-crytalline 4H-SiC Micro Cantilevers with a High Quality Factor", *Sensors and Actuators A: Physical*, vol. 197, pp. 122-125, 2013.
- [9] L. Jiang et al., "SiC Cantilever Resonators with Electrothermal Actuation", *Sensors and Actuators A: Physical*, vol. 128, pp. 376-386, 2006.
- [10] L. Belsito et al., "SiC Cantilever Resonators with Electrothermal Actuation", *Journal of Microelectromechanical Systems*, vol. 29, pp. 117-128, 2019.
- [11] F. Nabki et al., "Low-stress CMOS-compatible Silicon Carbide Surface-micromachining technology – Part II: Beam Resonators for MEMS above IC", *Journal of Microelectromechanical Systems*, vol. 20, pp. 730-744, 2011.
- [12] R. G. Azevedo et al., "A SiC MEMS Resonator Strain Sensor for Harsh Environment Applications", *IEEE Sensors Journal*, vol. 7, pp. 568-576, 2007.
- [13] K. Erbacher et al., "Investigation of Deep Dry Etching of 4H SiC Material for MEMS Applications Using DOE Modelling", in *2021 IEEE 34th International Conference on Micro Electro Mechanical Systems (MEMS)*, Gainesville, January 25-29, 2021, pp. 634-637.
- [14] K. Dowling et al., "Profile evolution of high aspect ratio silicon carbide trenches by inductive coupled plasma etching", *Journal of Microelectromechanical Systems*, vol. 26, pp. 135-142, 2017.
- [15] L. E. Luna et al., "Dry Etching of High Aspect Ratio of 4H-SiC Microstructures", *ECS Journal of Solid State Science and Technology*, vol. 6, pp. 207, 2017.
- [16] R. Liu et al., "A Dry Etching Method for 4H-SiC via Using Photoresist Mask", *Journal of Crystal Growth*, vol. 531, pp. 125351, 2020.
- [17] L. Ci et al., "Continuous Carbon Nanotube Reinforced Composites", *Nano Letters*, vol. 8, pp. 2762-2766, 2008.
- [18] D. N. Hutchison et al., "Carbon Nanotubes as a Framework for High-Aspect-Ratio MEMS Fabrication", *Journal of Microelectromechanical System*, vol. 19, pp. 75-82, 2009.
- [19] R. Poelma et al., "Tailoring the Mechanical Properties of High-Aspect-Ratio Carbon Nanotube Arrays using Amorphous Silicon Carbide Coatings", *Advanced Functional Materials*, vol. 24, pp. 5737-5744, 2014.

## CONTACT

\*J.Mo, tel: +31 630794557; J.Mo@tudelft.nl.